

See discussions, stats, and author profiles for this publication at: <https://www.researchgate.net/publication/26734969>

Marinopyrrole A Target Elucidation by Acyl Dye Transfer

ARTICLE in JOURNAL OF THE AMERICAN CHEMICAL SOCIETY · SEPTEMBER 2009

Impact Factor: 12.11 · DOI: 10.1021/ja903149u · Source: PubMed

CITATIONS

53

READS

47

6 AUTHORS, INCLUDING:



Yu-Liang Yang

Academia Sinica

61 PUBLICATIONS 1,220 CITATIONS

SEE PROFILE



Pieter C Dorrestein

University of California, San Diego

203 PUBLICATIONS 5,874 CITATIONS

SEE PROFILE



James La Clair

Xenobe Research Institute

91 PUBLICATIONS 1,476 CITATIONS

SEE PROFILE



William Fenical

University of California, San Diego

487 PUBLICATIONS 20,654 CITATIONS

SEE PROFILE

Published in final edited form as:

J Am Chem Soc. 2009 September 2; 131(34): 12094–12096. doi:10.1021/ja903149u.

Marinopyrrole A Target Elucidation by Acyl Dye Transfer

Chambers C. Hughes[†], Yu-Liang Yang[‡], Wei-Ting Liu[‡], Pieter C. Dorrestein^{‡,*}, James J. La Clair^{§,*}, and William Fenical^{†,*}

[†] Center for Marine Biotechnology and Biomedicine, Scripps Institution of Oceanography, University of California, San Diego La Jolla, CA 92093-0204, USA

[‡] Departments of Chemistry and Biochemistry, the Skaggs School of Pharmacy and Pharmaceutical Science, University of California, San Diego La Jolla, CA 92093-0204, USA

[§] Xenobe Research Institute, 3371 Adams Avenue, San Diego, CA 92164-4073

While a variety of methods exist,¹ target identification continues to pose a fundamental challenge in elucidating a natural product's mode of action.² The development of solutions to this problem is essential to advancing drugs into the discovery pipeline. The complex structural diversity that characterizes natural products complicates the adoption of routine protocols for these studies.³ A systematic approach to target elucidation would both facilitate the introduction of drugs into clinical trials, and challenge leads early on should undesired targets be identified.⁴

The process of determining the therapeutic mode of action of a natural product typically begins by developing probes bearing an affinity and/or fluorescent tag.⁵ The aim in this exercise is to construct a probe with activity comparable to its parent natural product. Often a loss in activity can be circumvented by use of bio-orthogonal approaches⁶ (Huisgen cycloaddition reactions or Click chemistry,⁷ Dielsalder cycloaddition,⁸ or olefin metathesis⁹), wherein the reporter is added bio-orthogonally after the natural product binds to its target. Though sufficient for cellular studies, the lack of a covalent link between the labeled natural product and its target commonly thwarts enrichment strategies (e.g., immunoprecipitation).

Crosslinking or photocrosslinking,¹⁰ a common solution to this problem, is frequently plagued by additional complications. First, the preparation of a dual-tag results in an enlarged probe,¹¹ which often exhibits only a fraction of the activity of its parent natural product.^{2b} Second, crosslinking methods are generally low yielding and unselective, increasing the complexity of downstream mass spectrometric (MS) analyses.¹² Finally, and perhaps most critically, the crosslinked target still bears a covalently linked natural product that is subject to xenobiotic metabolism (e.g., cytochrome P450 oxidation).¹³ Such metabolic processing leads to the formation of multiple products, each of which is detected by MS, obscuring subsequent protein identification and binding-site mapping studies. In the present study, the interaction of a natural product with its target(s) is addressed via an elimination or displacement reaction, wherein the natural product is removed from the reaction milieu, acting as a leaving group.¹⁴

Given the use of acyl phenols in protein reactive dyes,¹⁵ we examined the feasibility of this motif as a transfer agent for the immunoaffinity fluorescent (IAF) tag (Fig. 1a). Though the attachment of a phenol-containing linker would enable this method to be applied to natural

wfenical@ucsd.edu, pdorrest@ucsd.edu, or i@xenobe.org.

Supporting Information Available: Synthetic methods, copies of NMR spectra, protocols for cell imaging studies, IP studies and actin assays, detailed methods for the mass spectral studies, copies of original images in Figs. 2–3 as well as additional references are available free of charge via the Internet at <http://pubs.acs.org>.

products in a general sense, the marinopyrroles, a family of phenolic 1,3'-bipyrroles including **6** and **7**, were selected for this study.¹⁶ We chose these materials based on: (1) their availability from culture (strain CNQ-418) at mg/L scale, (2) their unknown mode of action, (3) their activity in tumor cell lines (GI₅₀ values for **6** and **7** were 10 μ M in HCT-116 cells and 620 and 500 nM for **6** and **7**, respectively, in A549 breast cancer cells) and (4) their *bis*-phenol structure, previously shown to undergo clean acylation to **8** with acetic anhydride (Scheme 1) without a loss in activity (GI₅₀ value of 0.8 μ M for **8** in HCT-116 cells, ~12 fold increase over **6** or **7**).¹⁶

Based on this evidence, *mono*-labeled **13** (45% yield) and *bis*-labeled **14** (traces) were prepared and analyzed using a combination of MS and NMR analysis. HMBC analysis confirmed the position of the tag in *mono*-labeled **14** (see Scheme 1). The low yield of the *bis*-labeled **14** was due to its instability, rapidly converting to **13** in aqueous media with a half-life $t_{1/2}$ = 40 min in PBS pH 7.2 at 32 °C. *Mono*-labeled **13** was much less prone to hydrolysis with a half-life of $t_{1/2}$ = ~2 d in PBS pH 7.2 at 32 °C.

Probes **13** and **14** mimicked the activity of marinopyrrole A (**6**). Probe **14**, with a GI₅₀ value of 1 μ M, was ~10 fold more active than the parent natural products **6** and **7**. Using two color confocal microscopy, we compared the native red fluorescence from marinopyrrole A (**6**) at 692 nm (Figs. 2a–2b) to the blue fluorescence from the IAF tag in **13** (Fig. 2d) and **14** (Fig. 2c). The presence of a similar pattern of red and blue staining confirmed that probes **13** and **14** shared the same subcellular localization in HCT-116 cells, and therefore provided a sufficient mimic of **6**. The co-localization of natural product **6** and dye-labeled probes **13** and **14** also showed that cells were not stained from the hydrolytic release of **9**. Importantly, control **12** was readily washed from cells under each study (insets, Fig. 2a–2d).

The putative protein target of the marinopyrrole probe was initially established using an immunoprecipitation (IP) protocol.^{2c} HCT-116 cells (~10⁸ cells) were incubated with 10 μ M **13** for 12 h. The cells were collected, lysed and screened for proteins that were labeled with the IAF tag. Two fluorescent bands at 40–45 kDa were apparent in the crude lysate (Fig. 3a). After IP, three bands were obtained (Fig. 3b). Mass spectral analysis (Fig. 3d) indicated that the two lower bands were actin, while the upper band arose from actinin. The fact that actinin was observed during IP experiments in the lysate, while not fluorescent, is expected given its tight complexation with actin.

The selective binding of the probe to actin was validated with purified proteins. Samples of rabbit muscle actin (Worthington Biochemicals) were treated with **13** or **14** to yield comparable fluorescently labeled bands (lanes L4-L7, Fig. 3e). Even with a 50-fold increase in concentration (lanes L1, L2, L3, L9 and L10 in Fig. 3e), the non-specific labels **10** and **11** failed to stain actin. The reactivity observed in Fig. 3e was indeed due to a specific binding event as pretreatment of actin with **6** effectively blocked the uptake of dye from **14** (lane L8, Fig. 3e).

Finally, mass spectral methods were applied to determine the site of dye transfer to actin. Protein from the reaction in lane L6 (Fig. 3e) was trypsin digested, purified by HPLC based on the absorbance of the IAF dye at 350 nm, and subjected to LTQ-MS/S with a NanoMate direct infusion system. Evaluation of the resulting spectra using the proteomics search tool, InSpecT, to find peptides that were modified by the IAF tag (M+286 Da), resulted in the identification of the modified peptide V₉₈APEEHPTLLTEAPLNPKANR₁₁₈. Because InSpecT annotated the modification to be anywhere from K₁₁₅ to R₁₁₈, we manually annotated the data to determine the site of localization. The manual annotation of the low-resolution data suggested that the modification could be found at K₁₁₅. To further improve the localization of the probe, the same sample was reanalyzed by LTQ-FTICR-MS, giving rise to a mass of 861.7839 Da within 6.6 ppm of the calculated mass of the modified peptide. Furthermore, all

the MS² b and y fragment ions observed by LTQ-FTICR-MS matched to within 0.02 Da enabling us to localize the site of modification to K₁₁₅. The unmodified peptide V₉₈APEEHPTLLTEAPLNPK₁₁₅ was also identified, which indicates that this residue was only partially modified.

Lysine 115 occupies a distinct site on actin (star, Fig. 4a) that does not overlap the ATP, gelsolin and profilin binding sites (see Supporting Information), nor does it overlap with the pocket targeted by other known natural products such as latrunculin A (dot, Fig. 4a), a marine natural product that binds to the nucleotide binding cleft of actin. Structural modeling identified a channel that exists adjacent to the amine terminus of K₁₁₅, suggesting a putative marinopyrrole-binding site (Fig. 4b–c).

Transfer of the IAF dye from the natural product to actin was further supported by secondary analyses. First, microcalorimetry analyses verified the binding between marinopyrrole A (**6**) and rabbit muscle actin with a K_d of 0.12±0.2 μM. The strength of this complex compares favorably to a reported value of 0.2 μM for latrunculin A (albeit at a different binding site, see Fig. 4a).¹⁷ Second, using a fluorescence assay (Cytoskeleton Inc.),¹⁸ **6** was shown to inhibit the polymerization of a pyrene-labeled G-actin with an IC₅₀ value of 39.5±6.2 μM (see Supporting Information). Lastly, actin fibers in live HCT-116 cells treated with probe **13** were blue fluorescent (Fig. 2f) from the binding of **13**, as evident by co-staining with FITC-phalloidin (Fig. 2e).

This investigation provides definitive support for the use of a dye transfer protocol via an acyl phenol motif for mode of action studies. By transferring the dye from the natural product to its protein target, we were able to streamline cellular, target elucidation, and binding site determination studies into a single workflow (see Fig. 1). Because bioactive natural products bind to proteins in selective binding pockets, the process of natural product mediated ligation may also be used to direct protein modifications site-specifically. Studies are now underway to evaluate the scope of this reaction centered on the electronic nature of the phenol and its ability to transfer its payload.

Supplementary Material

Refer to Web version on PubMed Central for supplementary material.

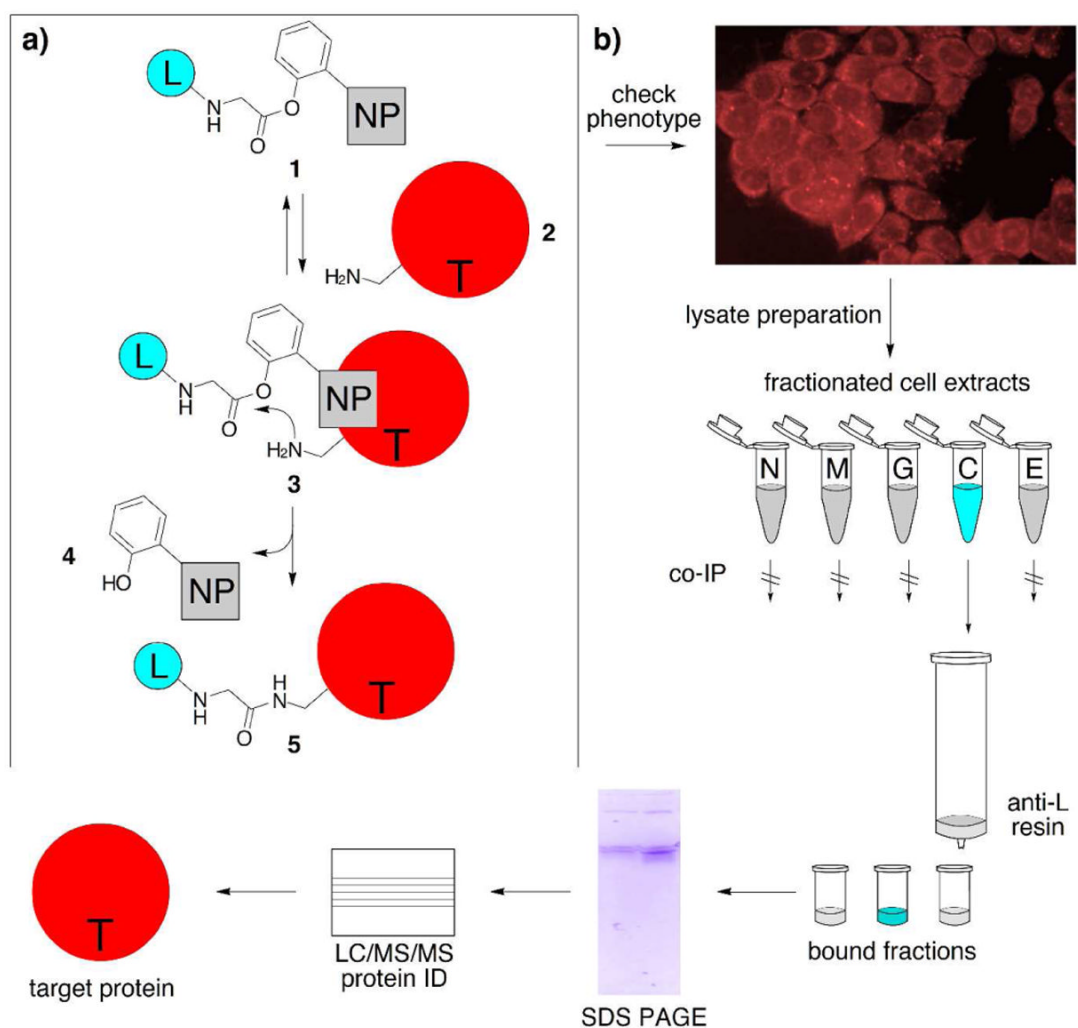
Acknowledgments

We thank Qishan Lin (CFG at University of Albany) for preliminary protein ID analyses. Support was provided by the NCI under grant R37 CA44848 (to WF), the V-foundation (to PCD) and NIH R01 GM086283 (to PCD).

References

1. (a) Leslie BJ, Hergenrother P. *J Chem Soc Rev* 2008;37:1347. (b) Wang X, Imber BS, Schreiber SL. *Bioconj Chem* 2008;19:585.
2. Recent examples: (a) Bowers A, West N, Taunton J, Schreiber SL, Bradner JE, Williams RM. *J Am Chem Soc* 2008;130:11219. [PubMed: 18642817] (b) Kotake Y, Sagane K, Owa T, Mimori-Kiyosue Y, Shimizu H, Uesugi M, Ishihama Y, Iwata M, Mizui Y. *Nat Chem Biol* 2007;3:570. [PubMed: 17643112] (c) Hughes CC, MacMillan JB, Gaudêncio SP, Fenical W, La Clair JJ. *Angew Chem Int Ed* 2009;48:728.
3. (a) Gough JD, Crews CM. *Ernst Schering Res Found Workshop* 2006;61. [PubMed: 16708999] (b) Drahl C, Cravatt BF, Sorensen EJ. *Angew Chem Int Ed Engl* 2005;44:5788. [PubMed: 16149114]
4. Altmann KH, et al. *ChemBioChem* 2009;10:16. [PubMed: 19115274]
5. (a) Peddibhotla S, Dang Y, Liu JO, Romo D. *J Am Chem Soc* 2007;129:12222. [PubMed: 17880073] (b) Alexander MD, et al. *ChemBioChem* 2006;7:409. [PubMed: 16432909]

6. (a) Carrico IS, Carlson BL, Bertozzi CR. *Nat Chem Biol* 2007;3:321. [PubMed: 17450134] (b) Sadaghiani AM, Verhelst SH, Bogoy M. *Curr Opin Chem Biol* 2007;11:20. [PubMed: 17174138] (c) Heal WP, Wickramasinghe SR, Leatherbarrow RJ, Tate EW. *Org Biomol Chem* 2008;7:2308. [PubMed: 18563263] (d) Channon K, Bromley EH, Woolfson DN. *Curr Opin Struct Biol* 2008;18:491. [PubMed: 18644449]
7. (a) Colombo M, Peretto I. *Drug Discov Today* 2008;13:677. [PubMed: 18675762] (b) Hein CD, Liu XM, Wang D. *Pharm Res* 2008;25:2216. [PubMed: 18509602] (c) Moorhouse AD, Moses JE. *ChemMedChem* 2008;3:715. [PubMed: 18214878]
8. (a) Weisbrod SH, Marx A. *Chem Commun* 2008;30:5675. (b) de Araújo AD, Palomo JM, Cramer J, Seitz O, Alexandrov K, Waldmann H. *Chemistry* 2006;12:6095. [PubMed: 16807971]
9. (a) Binder JB, Raines RT. *Curr Opin Chem Biol* 2008;12:767. [PubMed: 18935975] (b) Kirshenbaum K, Arora PS. *Nat Chem Biol* 2008;4:527. [PubMed: 18711379]
10. Tanaka Y, Bond MR, Kohler JJ. *Mol Biosyst* 2008;4:473. [PubMed: 18493640]
11. Guizzunti G, Brady TP, Malhotra V, Theodorakis EA. *Bioorg Med Chem Lett* 2007;15:320. [PubMed: 17110104]
12. Hurst GB, Lankford TK, Kennel SJ. *J Am Soc Mass Spectrom* 2004;15:832. [PubMed: 15144972]
13. (a) Dekant W. *EXS* 2009;99:57. [PubMed: 19157058] (b) Johnson WW. *Drug Metab Rev* 2008;40:101. [PubMed: 18259986]
14. During the preparation of this manuscript a team led by Hamachi disclosed a similar concept using ligand-directed tosylation: Tsukiji S, Miyagawa M, Takaoka Y, Tamura T, Hamachi I. *Nat Chem Biol* 2009;5:341. [PubMed: 19330012] (b) Tsukiji S, Wang H, Miyagawa M, Tamura T, Takaoka Y, Hamachi I. *J Am Chem Soc.* 2009early view
15. Gee KR, Archer EA, Kang HC. *Tetrahedron Lett* 1999;40:1471–1474.
16. Hughes CC, Prieto-Davó A, Jensen PR, Fenical W. *Org Lett* 2008;10:629. [PubMed: 18205372]
17. Coué M, Brenner SL, Spector I, Korn ED. *FEBS Lett* 1987;213:316. [PubMed: 3556584]
18. (a) Zhai LP, Panebra A, Guerrero AL, Khurana S. *J Biol Chem* 2001;276:36163. [PubMed: 11500485] (b) Pollard TD. *Anal Biochem* 1983;134:406. [PubMed: 6650826]

**Figure 1.**

Application of acyl dye transfer to natural product mode of action studies. a) A dye (L) labeled natural product (NP) probe **1** binds to target protein **2** forming complex **3**. Ligation-directed acyl transfer in complex **3** results in the displacement of phenol **4** and formation of labeled protein **5**. b) Typical workflow associated with antitumor mode of action studies on a natural product. The process begins by verifying the activity of the probe from a) in live cells. The process continues with steps that apply the probe for protein affinity purification or immunoprecipitation (IP) studies, gel analysis, and mass spectral based protein identification.

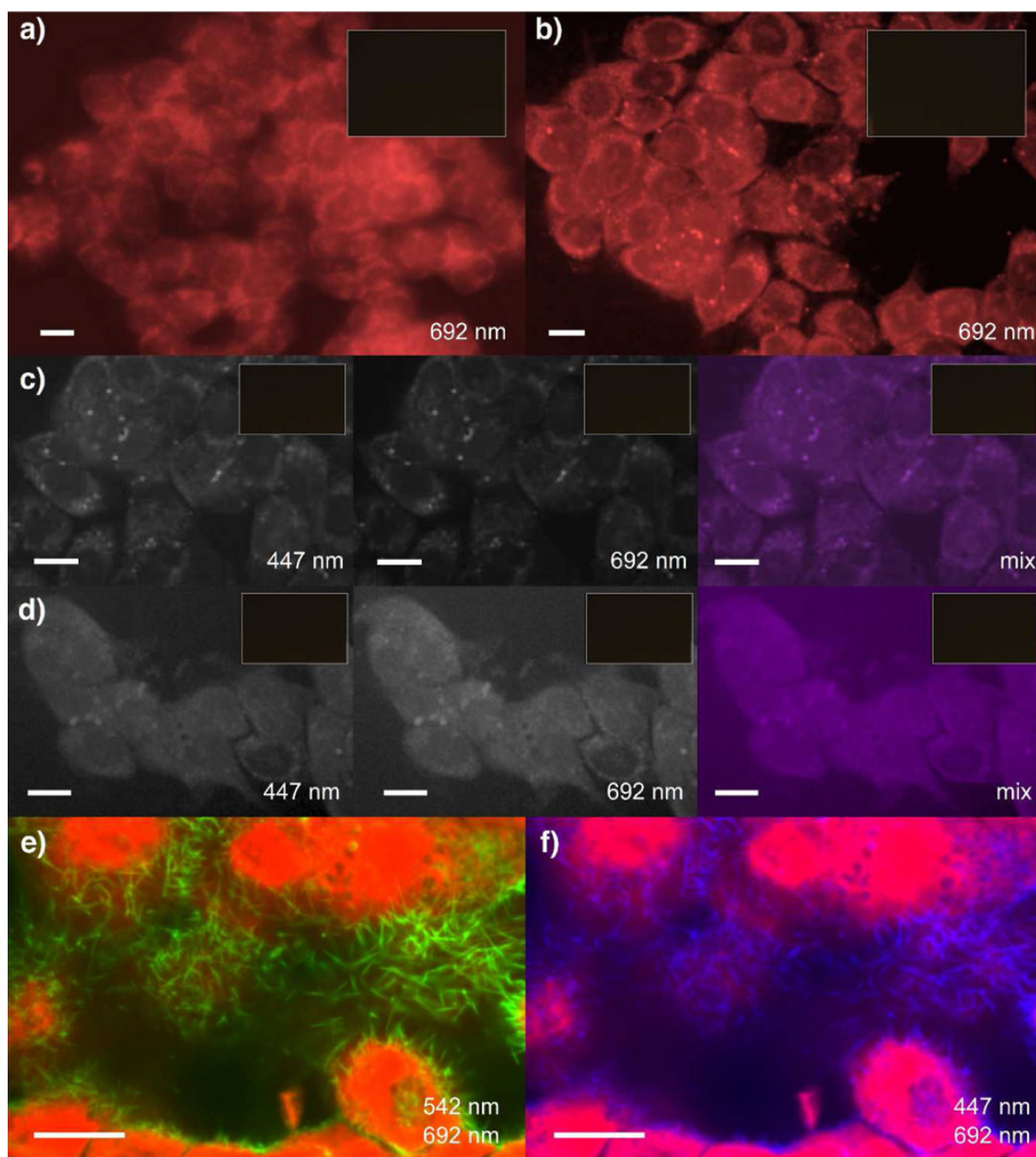
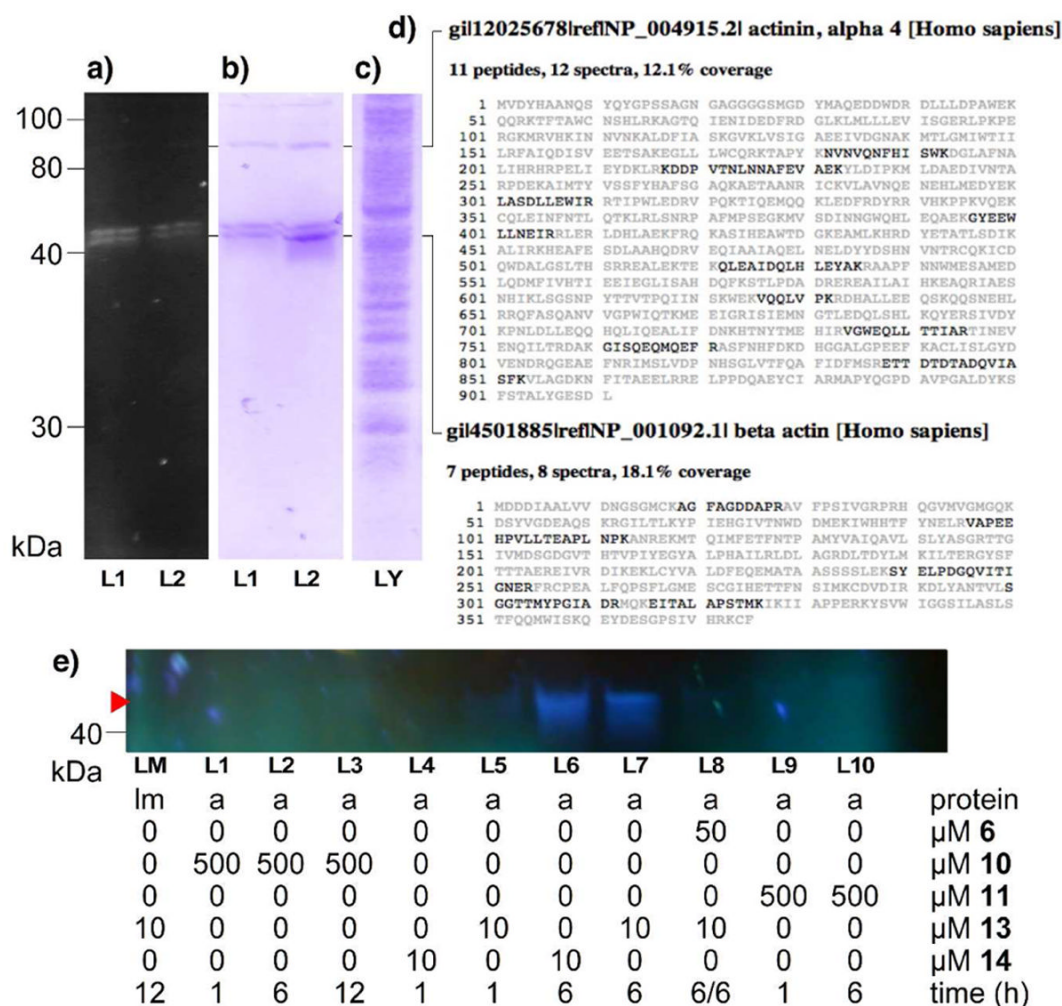


Figure 2.

Uptake and subcellular localization of probes **13** and **14** in HCT-116 cells. Confocal fluorescent images depicting the red fluorescence from the uptake of **6** in cells treated with a) 10 μM **6** for 1 h, or b) 10 μM **6** for 6 h. A set of confocal fluorescent images showing blue (447 nm), red (692 nm), and two color mixed (mix) fluorescence in HCT-116 cells treated with c) 10 μM **13** for 6 h, or d) 10 μM **14** for 6 h. Probe 14 likely hydrolyzed to **13** under these conditions. e) Image of cells treated with 10 μM **13** for 6 h and then washed, fixed and stained for nucleic acids with Syto-60 (red) and actin with FITC-phalloidin (green). f) Identical cells as in e) stained for nucleic acids (red) and transfer of the IAF tag to actin (blue). Note the overlap of green in e) with blue in f). All cells were treated under conditions wherein control **12** was

completely washed from cells (inset images). Wavelengths denote the center of emission filter. Bars denote 10 μm .

**Figure 3.**

Marinopyrrole probes target actin. a) A fluorescent gel showing cell lysate obtained from HCT-116 cells (10^8 cells) treated with $10 \mu\text{M}$ **13** in L1 and $10 \mu\text{M}$ **14** in L2 for 12 h. b) A Silver Blue stained SDS-PAGE gel depicting proteins immunoprecipitated from the lysate in a) using Affigel 10 resin containing 3.5 mg/mL of an anti-IAF antibody XRI-TF35. c) SDS-PAGE gel depicting the HCT-116 cell lysate used in b). d) LC/MS/MS analysis of the IP product in b) containing actin and actin binding proteins. e) A fluorescent SDS-PAGE gel of $5 \mu\text{M}$ rabbit muscle actin (protein = a, lanes L1-L10) treated with IAF tags **10–11** and probes **13–14** at 32°C . Reactions were conducted under conditions wherein probe **13** did not label a lane marker (NativeMark, Invitrogen. protein = lm, lane LM). Fluorescent gels were imaged by excitation at 360 nm.

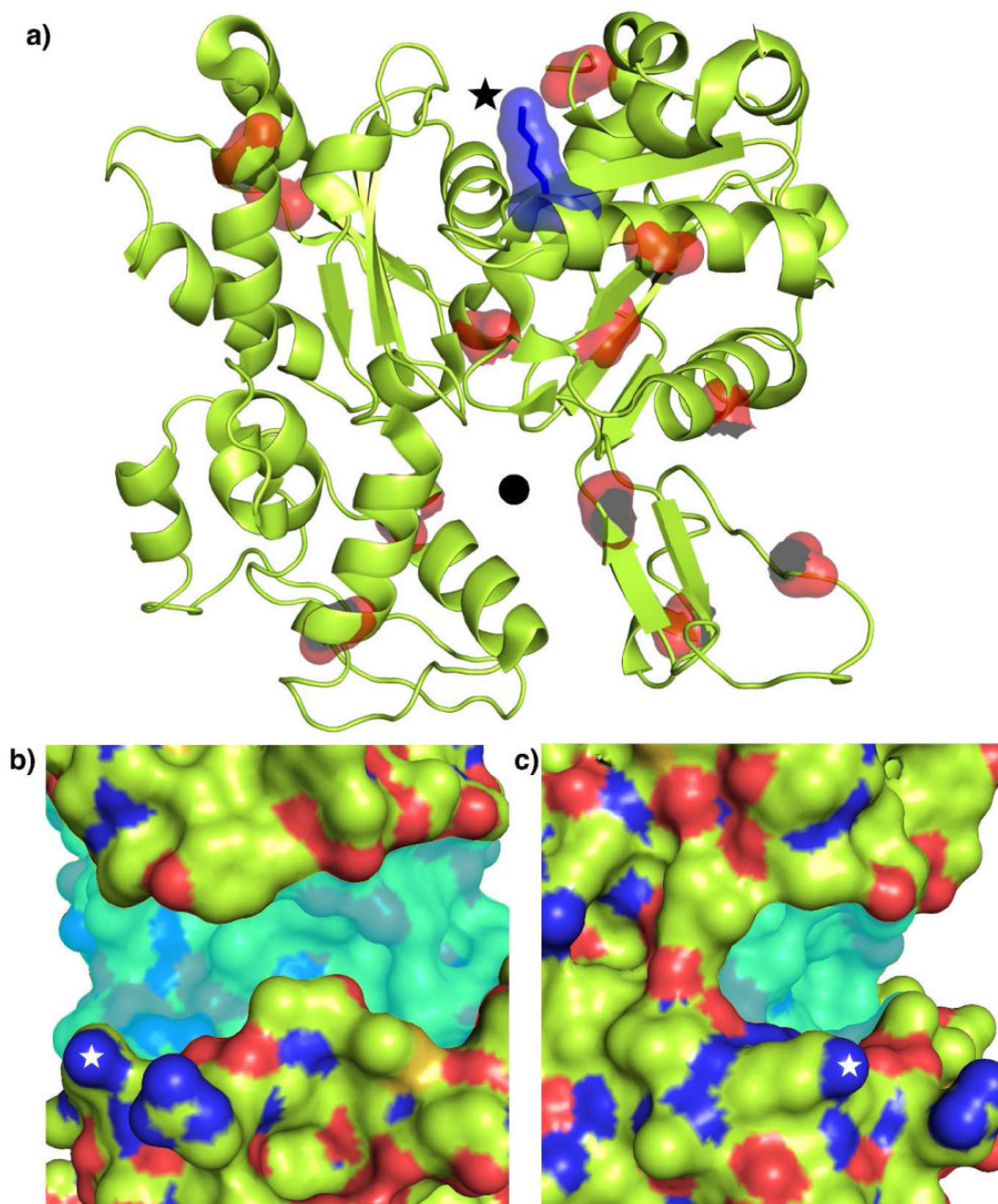
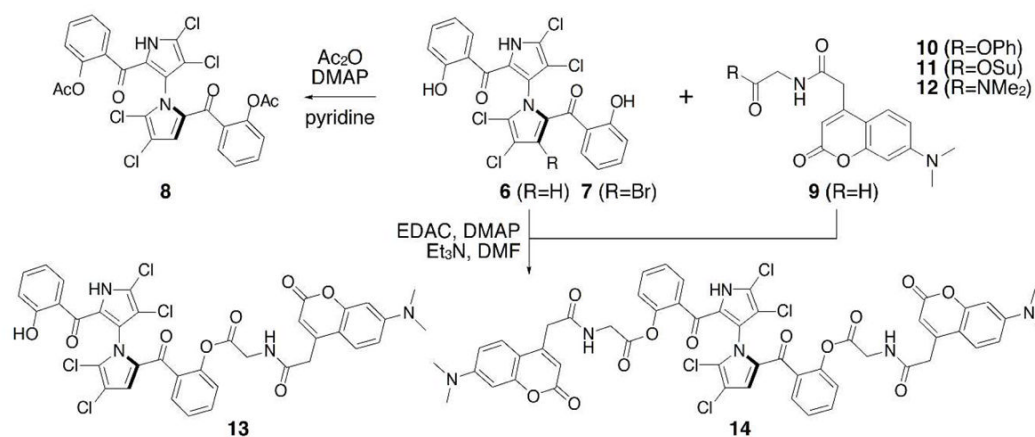


Figure 4.

Marinopyrrole probe **13** transfers an IAF tag selectively to residue K₁₁₅ of actin. a) Structure of actin (green) noting the position of the targeted K₁₁₅ residue (blue) and other lysine residues (red). b) Side and c) frontal views of the putative marinopyrrole binding pocket (aqua shaded). Images were developed using a complex between rabbit skeletal muscle actin and latrunculin A at 2.85 Å (pdb id: 1IJJ). The side chain amine of K₁₁₅ (star) and the latrunculin A binding pocket (sphere) are noted.

**Scheme 1.**

Structures of marinopyrrole A (6) and marinopyrrole B (7), IAF labels 9–11, control 12 and the synthesis of *bis*-acetate 8, *mono*-labeled probe 13 and *bis*-labeled probe 14.